



Research Article

# DGS based monopole circular-shaped patch antenna for UWB applications

Dattatreya Gopi<sup>1</sup> · Appala Raju Vadaboyina<sup>2</sup> · J. R. K. Kumar Dabbakuti<sup>3</sup>

Received: 30 April 2020 / Accepted: 30 December 2020 / Published online: 25 January 2021  
© The Author(s) 2021

## Abstract

A simple low profile defected ground structure based monopole circular-shaped patch antenna is proposing for ultrawide-band applications. The design allows for a simple and compact structure on the FR-4 substrate material. The proposed design initially has a meager antenna gain and bandwidth. To increase the antenna bandwidth and gain, the defective ground structure is implemented with four dumble-shaped slots. Parametric analysis is considered to find the radius of circular patch for tuning of UWB frequency applications. The proposed MCP antenna resonates at 2.9 GHz, 9.1 GHz frequencies with a  $S_{11}$  of  $-34.84$  dB,  $-33.74$  dB, respectively, and achieves 8.1 GHz (2.5–10.6 GHz) impedance bandwidth concerning the  $-10$  dB reference line of the reflection coefficient. The gains are 8.4 dBi, 8.2 dBi for the two resonant frequencies, and the radiation patterns are semi-omnidirectional, omnidirectional. The proposed antenna has been validated by observing good agreement between the simulation and the measured results.

**Keywords** Circular patch · Defected ground structure (DGS) · Monopole · Ultra-wideband (UWB) · Wireless applications

## 1 Introduction

Ultrawide-band (UWB) technology fascinated academia and industry focus on the wireless world since the federal communications commission (FCC) has officially assigned the 3.1–10.6 GHz spectrum to UWB communications applications in 2002 [1]. The extensive release of the 3.1–10.6 GHz spectrum for commercial applications has generated much interest in short-range wireless communications and the development of UWB technology for wireless applications, mage radar, remote sensing, location confirmation applications. The UWB antenna design's primary purpose is to reduce manufacturing efficiency, increase gain, and secure a wide bandwidth while maintaining good radiation efficiency. The compact [2] and low profile antenna [3] system is a unique role over traditional narrowband systems. Also, thin, lightweight, and easy to

manufacture planar UWB antennas have received much attention to providing easy wireless access to multimode communication systems. A printed monopole antenna is manufactured on a substrate with a wide bandwidth that can cover UWB. In [4], a monopole circular ring-shaped antenna is proposed for UWB applications. Different shapes like rectangular, circular, elliptical, and curved monopole antennas have been reported in [5–8] to achieve UWB. There are a variety of shapes that can be used to design microstrip patches for example, dipoles, squares, rectangles, triangles, circles, circular rings, ring sectors, disk sectors. Circular patches have advantages such as design flexibility and have the highest bandwidth in GHz and provide acceptable lossy characteristics, enhanced gain, desirable electric field, and magnetic field strength patterns.

✉ Dattatreya Gopi, dattatreya.gopi@gmail.com | <sup>1</sup>Department of Electronics and Communication Engineering, Raghu Engineering College, Visakhapatnam, A.P, India. <sup>2</sup>Department of Electronics and Communication Engineering, Vignan's Institute of Information Technology, Visakhapatnam, A.P, India. <sup>3</sup>K L E F, K L Deemed To Be University, Guntur, A.P, India.



The desirable characteristics of circular patch antennas can be enhanced by introducing slots, defective grounding structures [9]. A monopole circular-shaped patch antenna [10] is proposed with a pentagonal slot for UWB applications. To modify the circular patch antennas for better results, researchers propose antennas by introducing a taper in shape [11], the slot method [12, 13]. Some of these shapes were used in the form of rings and patches [14]. In particular, circular discs and rectangular monopole antennas have been extensively studied due to their simple construction. A band notch characteristic can be obtained by introducing a pair of an open slit, a dielectric resonator [15], a dumbbell [16] at the ground plane, and changing the angular separation between slits of a circular patch [17]. Sometimes segments (quadratic shaped) are introduced not only in the ground plane but also in patch element [18] by providing tapered feeding get the ultra-wideband (UWB) in CP printed antenna [19]. The introduction of slots into radiating patches, defective ground plane structures due to slots, and taper on the ground plane were also investigated [20]. To improve the CP antenna characteristics, a DGS is also taken into account [21]. Monopole fork-shaped [22], arc-shaped patches with parasitic rectangle patches [23] are used to obtain UWB frequencies. Multiband frequencies are obtained by a modified circular radiating patch and two I-shaped slots with the top corners cut off on the antenna's ground plane [24]. In [25], UWB reconfigurable circular ring patch antenna is proposed. CPW-fed UWB antenna [26] based on concentric circle packing is proposed for circular patches. Therefore, the introduction of the DGS has greatly improved the frequency characteristics of the antenna.

In this paper, a simple MCP antenna is proposed for UWB applications. UWB resonance characteristics obtained by creating a circular shaped patch on top of the substrate and creating a defective ground plane with a dumbbell slot on the bottom side of the substrate. Details of the antenna design can be found in Section 2. Section 3 shows the antenna characterization with simulation results. Results and discussion are explained in Section 4. Finally, the conclusions are explained in Section 5.

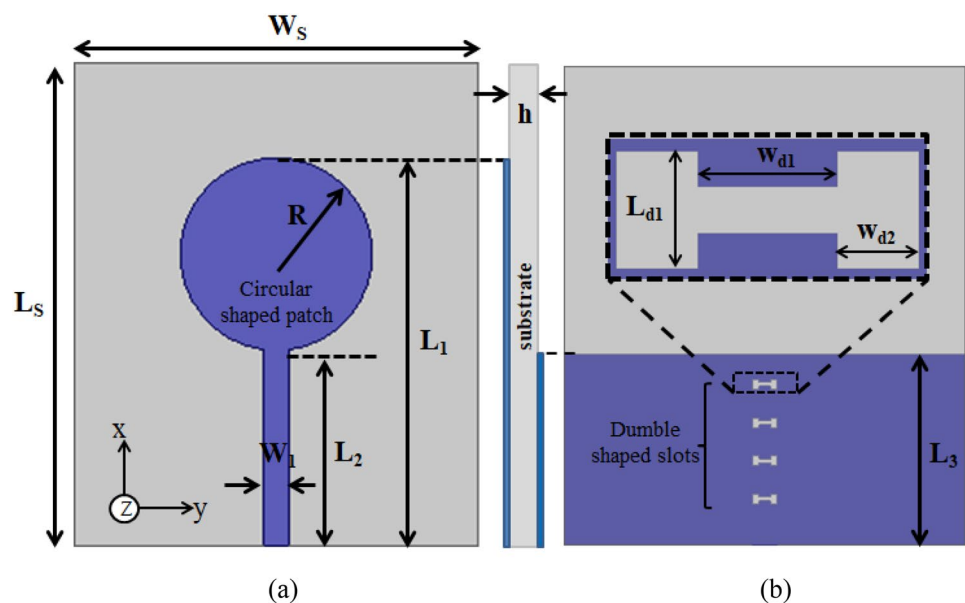
## 2 Antenna design

The MCP antenna geometry is shown in Fig. 1. The MCP antenna is having dimensions of substrate (FR-4 epoxy) length  $L_s = 48$  mm, width  $W_s = 38$  mm, and  $h = 1.6$  mm with  $\epsilon_r = 4.4$ , and loss of tangent ( $\tan\delta$ ) is 0.02. A circular patch antenna having radius  $R = 10$  mm is mounted on a surface of the substrate, and providing  $50 \Omega$  microstrip feed line is depicted in Fig. 1

The circular monopole patch and stripline lengths are considered as  $L_1 = 40$  mm,  $L_2 = 20$  mm with stripline width  $W_1 = 2$  mm. To enhance the bandwidth, defected ground structure (DGS) is considered on the bottom side of the substrate material. The length of the ground is  $L_3 = 20$  mm. As shown in Fig. 1b, four dumbbell shaped slots are considered on the DGS plane with the dimensions of  $L_{d1}$ ,  $W_{d1}$ ,  $W_{d2}$  as 1 mm, 1.2 mm, 0.7 mm, respectively.

The radius 'R' (Eq. (2)) of the circular patch is calculated by using effective radius  $R_{eff}$  (Eq. (1)) [27].

**Fig. 1** Geometry of monopole circular-shaped patch antenna **a** top view, **b** bottom view



$$R_{eff} = \frac{8.79 \times 10^9}{f_{res} \sqrt{\epsilon_r}} \tag{1}$$

$$R = \frac{R_{eff}}{\left(1 + \frac{2h}{\pi \epsilon_r R_{eff}} \left[ \ln\left(\frac{1.57 R_{eff}}{h}\right) + 1.78 \right]\right)^2} \tag{2}$$

where  $f_{res}$  is the first resonant frequency,  $\epsilon_r$  is the dielectric constant of the substrate material.

### 3 Antenna characterization

The antenna evolution process is done by considering circular and square patches connecting to the feed line. The diameter of the circular patch is taken as 20 mm, and the length of the square patch is considered as 20 mm. The simulated reflection coefficient ( $S_{11}$ ) plot is shown in Fig. 2. It is observed that the circular patch connected to the 50Ω impedance line will resonate at two operating frequencies with UWB.

DGS is used to design compact structures with enhanced bandwidth and gain. The fabrication process is also easier compared to other bandwidth and gain enhancing techniques. Generally, the geometry of DGS consists of one or a few slots. To achieve UWB with improved antenna performance, more than two slots are considered in DGS for the proposed MCP antenna. DGS below the microstrip feed line modifies the capacitance and inductance of the feed line by considering the resistance, inductance, and capacitance of slots. The equivalent circuit diagram of a dumbbell shaped slot [28] is shown in Fig. 3.

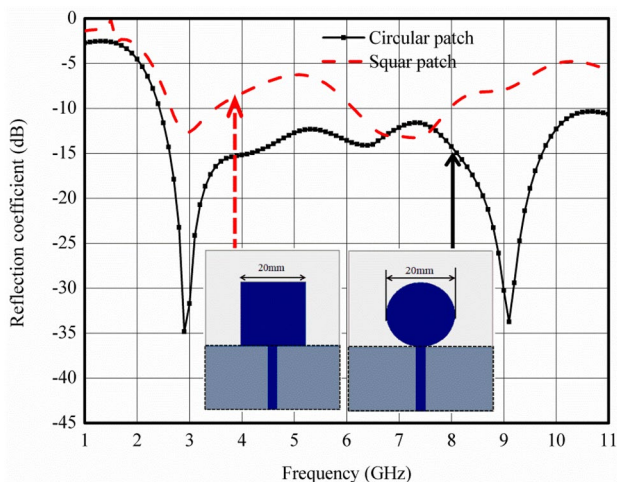


Fig. 2 The evolution process of the monopole circular-shaped patch antenna with Reflection coefficient ( $S_{11}$ ) response

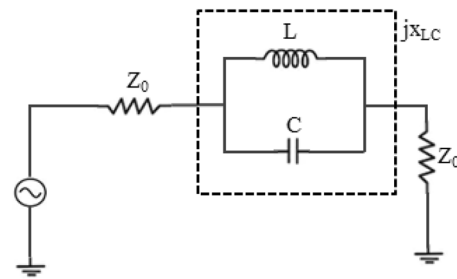
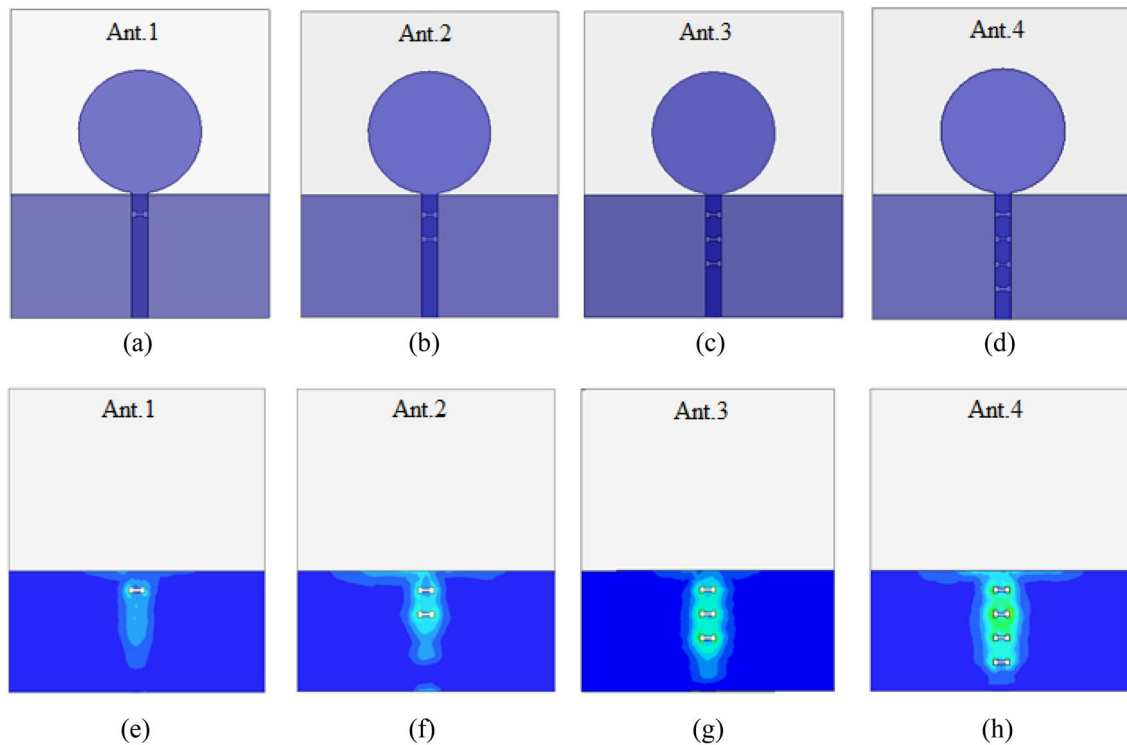


Fig. 3 Equivalent circuit diagram of dumbbell shaped slot DGS

Figure 4 shows the evolution process and radiation intensity of DGS. For the first evolution process, only one dumbbell shaped slot is considered on a partial ground plane. Ant. 1 resonates at 3 GHz and 9.3 GHz frequencies with a  $S_{11}$  of  $-38.6$  dB and  $-35.9$  dB, respectively. The gains are observed as 5.64 dBi and 7.08 dBi for the Ant. 1. In the second evolution process, two dumbbell shaped slots are considered with proper spacing, and the obtained frequencies are 3 GHz, 9 GHz with  $S_{11}$  of  $-34.9$  dB, and  $-28.2$  dB. There is a shift in frequency is observed for the second resonant frequency from the first evolution to the second, and also the gains are improved to 6.37dBi, 7.17 dBi.

The third evolution process includes three dumbbell shaped slots on the partial ground plane, and the frequencies are 3 GHz and 9.2 GHz, with  $S_{11}$  observed as  $-41.9$  dB and  $-38.3$  dB, respectively. The bandwidths are separated for the two resonant frequencies by the  $-10$  dB reference line, as shown in Fig. 5, for evolution 1 (Ant. 1) to evolution 3 (Ant. 3). The final evolution four dumbbell shaped slots are arranged with equal distance to get the desired UWB with the resonating frequencies 2.9 GHz, 9.1 GHz, and  $S_{11}$  of  $-34.84$  dB,  $-33.74$  dB, respectively. The periodic dumbbell shaped slots arrangement will lead to improved antenna performance. The overall performance for each evolution process is tabulated in Table 1. By considering the DGS, the desired UWB is obtained. As the number of slots increases in DGS, the radiation intensity is concentrated on the slots, as shown in Fig. 4e–h. The reflection coefficient response of the MCP antenna with and without DGS is shown in Fig. 5.

The radius (R) of the circular disc and length ( $L_3$ ) of the ground plane are two important design parameters that affect the antenna performance. Figure 6 represents the  $S_{11}$  response of the MCP antenna with different values of R. It is observed from the plot that the desired UWB is obtained by considering the radius of the circular disc as 10 mm. For the other values of radius, the bandwidth is limited.



**Fig. 4** Monopole circular-shaped patch antenna evolution process with DGS

**Table 1** Performance analysis of MCP antenna for DGS evolution

S. no	No. of dumble shaped slots on DGS	Obtained frequencies (GHz)	Reflection coefficients (dB)	Bandwidth (GHz)	Simulated gain (dBi)
1	One	3	-38.6	2.6-7.1	5.64
		9.3	-35.9	7.15-10.1	7.08
2	Two	3	-34.9	2.6-7.2	6.37
		9	-28.2	7.26-10.12	7.17
3	Three	3	-41.9	2.5-7.2	6.38
		9.2	-38.3	7.22-10.2	6.69
4	four	2.9	-34.84	2.5-10.6	8.4
		9.1	-33.74		8.2

### 4 Results and discussion

The design and simulations are performed using Ansys HFSSv19 tool, which utilizes the finite element method. The optimized antenna is fabricated with a Nivas75 milling machine to verify the measured results. The photographs of the fabricated MCP antenna are presented in Fig. 7. The reflection coefficient ( $S_{11}$ ) is measured with a ZNB-20 R&S vector network analyzer. The measurement result is similar to the simulation result. The results may show slight discrepancies between measurement and simulation due to manufacturing errors. Also, due to the influence of the coaxial cable used for measurement, a

deviation has occurred. On the other hand, simulations do not allow mismatches.

With DGS, the simulated  $S_{11}$  covers a bandwidth of 8.1 GHz (2.5-10.6 GHz) with  $RL \geq -10$  dB. Dumble slots improve the impedance matching enhance the bandwidth and gain. The obtained bandwidth useful for many wireless applications. The 3.5 GHz band is for IMT services, 3.3-3.8 GHz is for WiMAX applications, 5.15-5.35 GHz and 5.725-5.825 GHz for WLAN applications, 2-4 GHz and 4-8 GHz for satellite communications, etc. The proposed antenna excels in the similarity between simulation and measurement results, as shown in Fig. 8 by comparing the simulation results, the measurement results are much better in the 2.5 GHz to 10.6 GHz range.

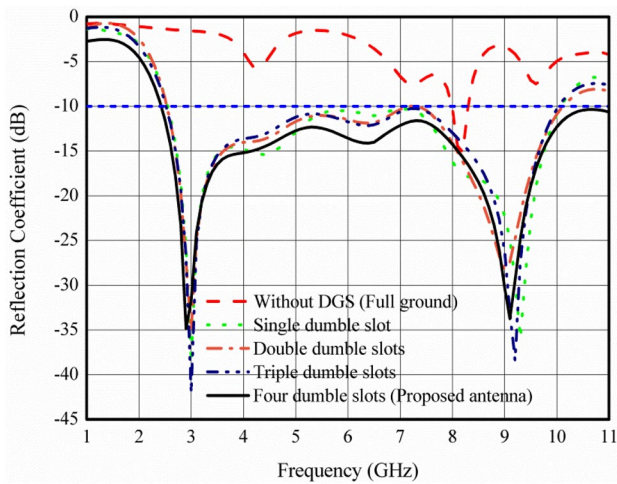


**Fig. 5** The Reflection coefficient ( $S_{11}$ ) of the monopole circular-shaped patch antenna with and without DGS

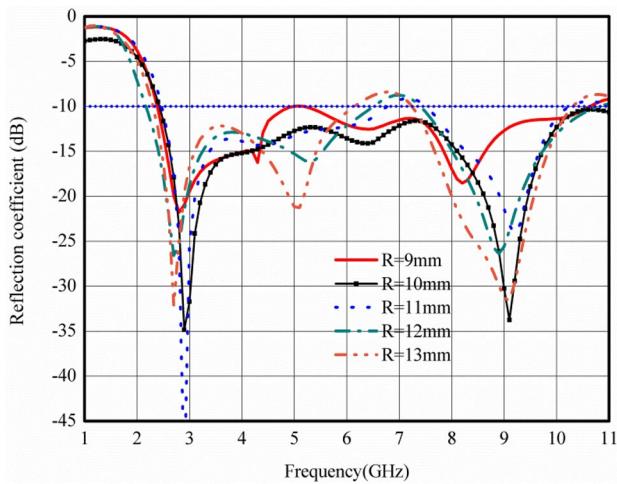


**Fig. 6** Reflection coefficient ( $S_{11}$ ) response for different values of ‘R’ of monopole circular-shaped patch antenna

The comparison of simulated and measured  $S_{11}$  is shown in Table 2. It is observed that good agreement is observed between simulated and measured  $S_{11}$ . The bandwidths are observed 8.1 GHz for simulated and 11.97 GHz for measured  $S_{11}$

Gain transfer method is one of the most common techniques to measure the gain. In this method, three antennas are to be considered. They are transmitting antenna (AARONIA-AG Power LOG70180 Horn Antenna), Reference antenna (standard gain), Antenna under Test (AUT). The gain of the proposed antenna is measured by using Eq. (3) [27]. The gain measurement setup of MCP antenna is shown in Fig. 9. The measured peak gains are observed as 8.3dBi and 7.9dBi for the 2.9 GHz and 9.1 GHz frequencies. The deviations in simulated and

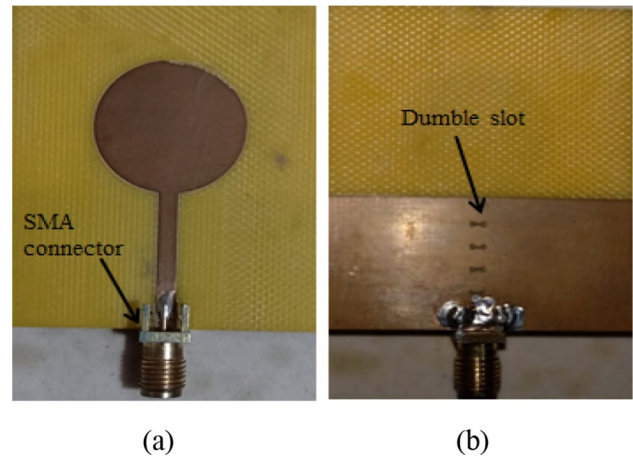


**Fig. 7** Fabricated model of monopole circular-shaped patch antenna. **a** Top view, **b** bottom view

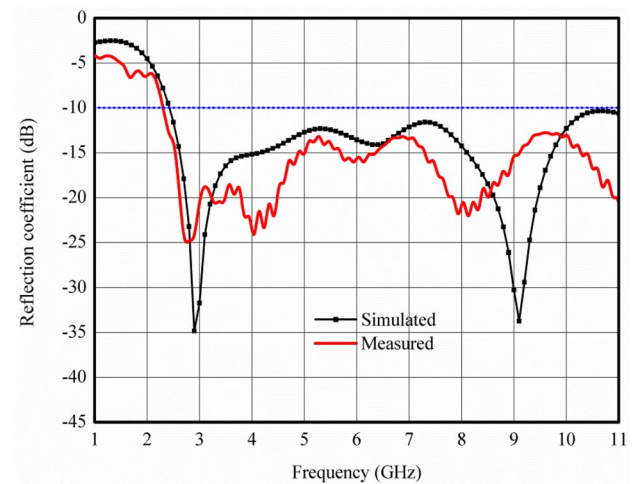


**Fig. 8** The simulated and measured reflection coefficient ( $S_{11}$ ) of the monopole circular-shaped patch antenna

**Table 2** Comparison of simulated and measured reflection coefficient ( $S_{11}$ ) of the MCP antenna

Measurement	$S_{11}$	Operating frequency (GHz)	Bandwidth (GHz)
Simulated	$\geq -10$ dB	2.5–10.6	8.1
Measured	$\geq -10$ dB	2.33–14.3	11.97

measured gains are occurred due to the cable and connecting losses.

$$G_{AUT} = G_{Ref} + 10 \log_{10} \left[ \frac{P_{AUT}}{P_{Ref}} \right] \tag{3}$$

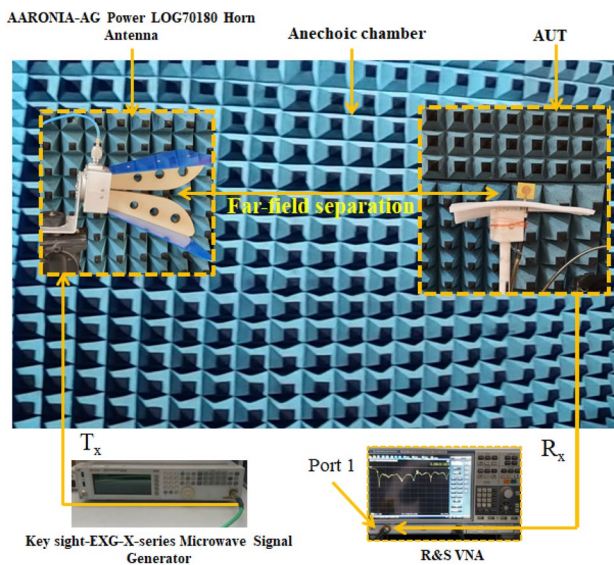


Fig. 9 Gain measurement setup of the proposed MCP antenna

where  $G_{AUT}$  is the gain of the antenna under test,  $G_{Ref}$  is the standard gain of reference antenna,  $P_{AUT}$  is the power received with the antenna under test,  $P_{Ref}$  is the power received with the standard gain antenna.

The simulated 3D-gains of the MCP antenna is shown in Fig. 10 and are observed 8.4 dBi, 8.2 dBi for the two resonant frequencies in the bandwidth of 2.5–10.6 GHz. In Fig. 10b, due to the higher frequency of 9.1 GHz, the

higher-order current mode excitation causes the gain pattern to be directional and some nulls.

The radiation efficiency of the MCP antenna is shown in Fig. 11. The radiation efficiency is observed as 90.27% for the 2.9 GHz frequency and 86.17% for the 9.1 GHz resonant frequency. For the entire bandwidth of 2.5 GHz–10.6 GHz the efficiencies are in-between 85 and 91%. The radiation efficiency and gain are influenced by the lossy dielectric substrate materials. By using a loss less microwave substrate materials, the radiation efficiencies and the gains of the proposed MCP antennas can be improved.

The surface current distributions and the axial ratio plots are considered to demonstrate polarization of the MCP antenna. The axial ratio of the MCP antenna is shown in Fig. 12. It is clear from the plot that the antenna exhibits a 3 dB axial-ratio bandwidth of 23.3% for the 2.9 GHz frequency band and attains a minimum value at 9.1 GHz with a bandwidth of 3.2% which is within the impedance bandwidth.

The normalized 2D simulated radiation patterns of the proposed MCP antenna in co-polarization (co-polar) and cross-polarization (X-polar) radiated fields are shown in Fig. 13a, b, respectively in the E-plane ( $\phi = 0$ ) and H-plane ( $\phi = 90$ ). In Fig. 13a, the X-polar is lower for the 2.9 GHz frequency. In E-plane the X-polar magnitudes are less than 20 dB compared to the co-polar magnitudes at  $90^\circ$  and  $270^\circ$ , the X-polar magnitude is observed 8 dB low at  $90^\circ$  compared to Co-polar in H-plane for 2.9 GHz frequency. It can be observed that at the low frequency of 2.9 GHz,

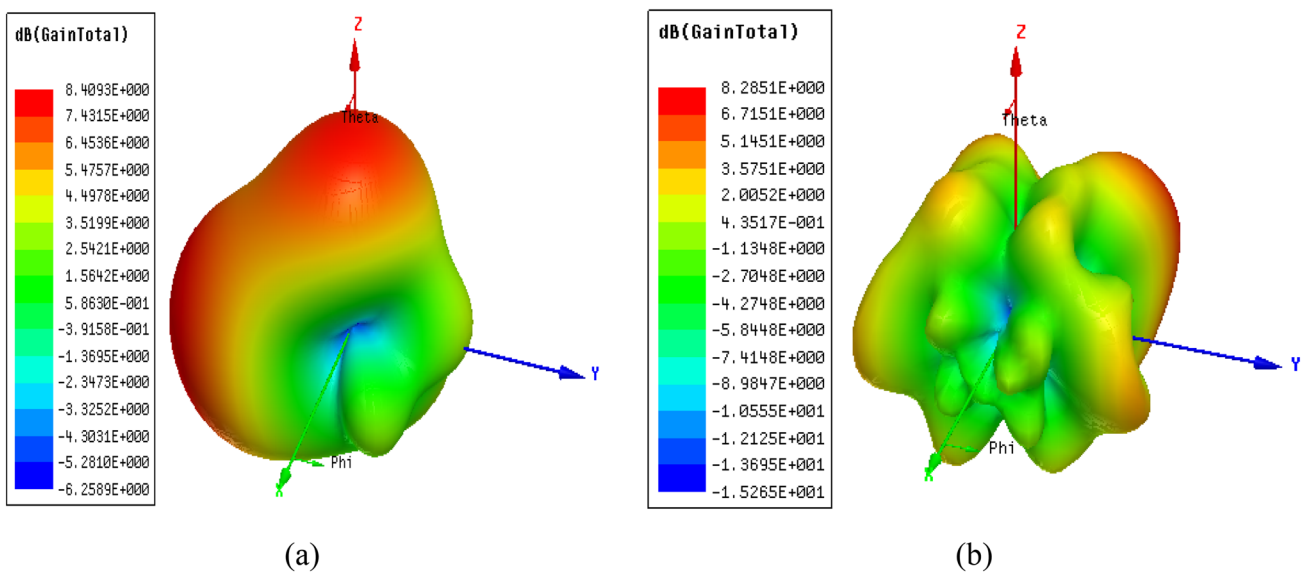
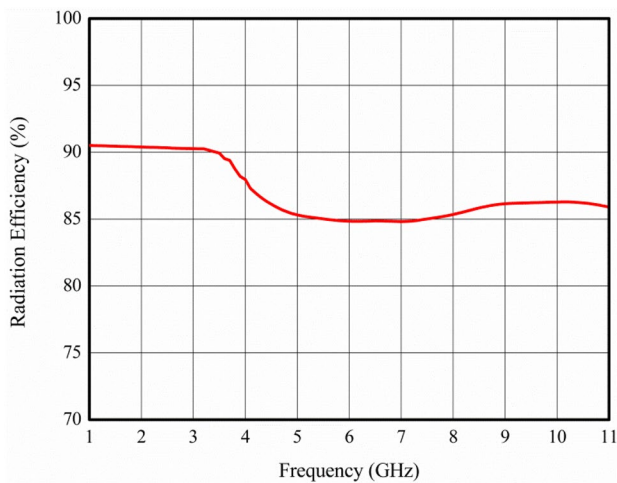
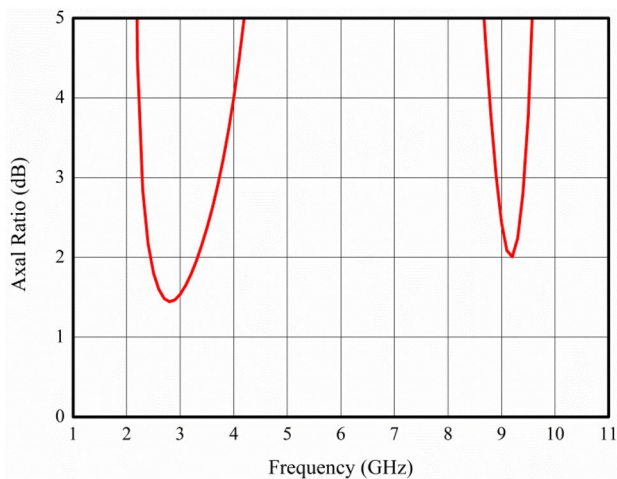


Fig. 10 Gain (dBi) of monopole circular shaped patch antenna at **a** 2.9 GHz, **b** 9.1 GHz frequencies



**Fig. 11** Radiation efficiency of monopole circular shaped patch antenna



**Fig. 12** Axial Ratio of monopole circular shaped patch antenna at 2.9 GHz and 9.1 GHz frequencies

the radiation patterns are omnidirectional. At a higher frequency of 9.1 GHz, the radiation pattern is still approximately omnidirectional, but the X-polar levels are high in the 9.1 GHz resonance frequency due to higher harmonics. By observing the radiation characteristics, the proposed MCP antenna radiates in all directions with a good magnitude.

Figure 14 shows the simulated surface current distribution at the 2.9 GHz frequency. The maximum current intensity of 117.5A/m is focused on the edge of the disc

and feed line. Some of the intensity is also observed at the dumbbell shaped slots on the ground plane. The surface current distributions are also observed at different phase angles  $0^\circ$ ,  $90^\circ$ ,  $180^\circ$ ,  $270^\circ$ ,  $360^\circ$ . For  $0^\circ$  and  $180^\circ$  phase angles the feed line and the lower part of circular patch carries a large current distribution. The current distributions are also observed in feed line and circular patch edges with a circular rotation for  $90^\circ$  and  $180^\circ$  phase angles. For  $270^\circ$  phase angle, again the rotated currents are distributed on feed line.

Figure 15 shows the surface current distribution of the MCP antenna at the 9.1 GHz frequency. It can be observed that the feeding line carries a large amount of current. At this point, the electric field has been generated. On the ground plane, the current is mainly distributed on the slotted line. That is, the part of the ground plane that returns to the feeder acts as part of the radiating structure. The surface current distribution is observed at various phase angles of  $0^\circ$ ,  $90^\circ$ ,  $180^\circ$ ,  $270^\circ$ ,  $360^\circ$ . The surface current distributions are observed at some portions of the feed line, circular patch for both  $0^\circ$  and  $360^\circ$  phase angles. For  $90^\circ$  to  $270^\circ$  the surface current distributions are rotated in a circular manner. In  $90^\circ$  the maximum intensity is observed at the feed line, and for  $180^\circ$ ,  $270^\circ$  the intensity is concentrated at both the feed line and circular disc.

Table 3 illustrates a comparison of antenna size, reflection coefficient, resonating bands, bandwidth, and gains of the MCP antenna with other models. Previously proposed models used the partial ground plane without any slots [5–7, 14, 20]. The bandwidths can be enhanced with radiating patches of circular, tapered, edge curved, elliptical-shaped radiating patches without slots. In [4, 10, 11, 22, 23] has used a single slot on the partial ground plane to enhance the proposed antenna bandwidth. The aforementioned models are good in applications for improving bandwidth. The proposed MCP antenna with periodic dumbbell shaped slots on the partial ground plane antenna show advantages in terms of bandwidth enhancement and improve the overall performance of the antenna without changing the dimension of the antenna.

The major limitation of the proposed MCP antenna is the proper spacing and placing of dumbbell shaped slots. The periodic DGS is considered below the feed line, which modifies the capacitance and inductance of the feed line by considering the resistance, inductance, and capacitance of slots. However, when integrating this type of antenna with a printed circuit board, it is advisable to place the RF circuitry away from the ground plane to avoid spurious emissions.

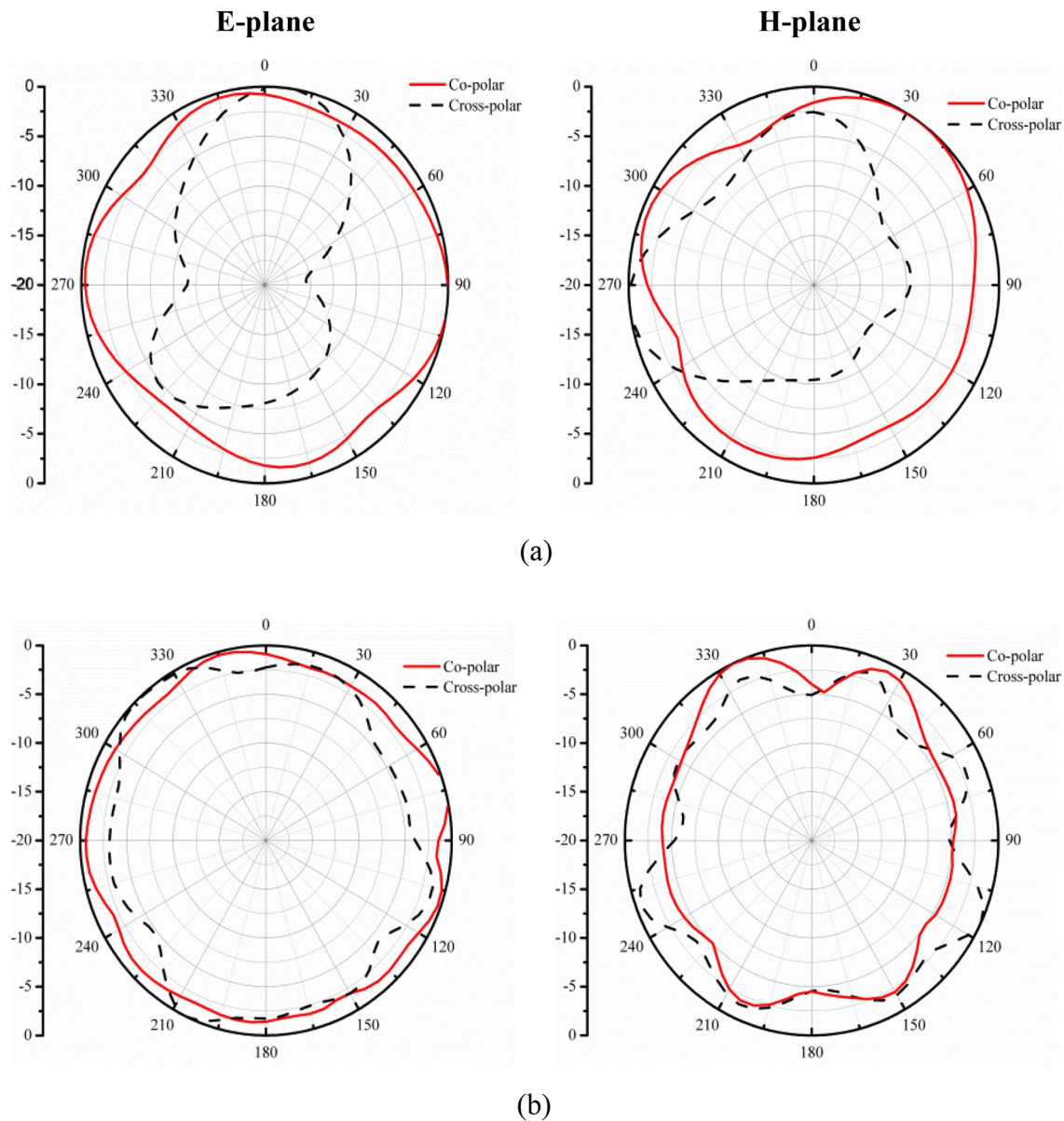


Fig. 13 E-plane and H-plane normalized radiation patterns of proposed antenna at **a** 2.9 GHz, **b** 9.1 GHz

### 5 Conclusion

A simple low profile monopole circular patch (MCP) antenna ( $38 \times 48 \times 1.6 \text{ mm}^3$ ) has been successfully implemented in the FR4 substrate for UWB applications. Bandwidth and gains are improved by using a defective ground structure on the bottom of the substrate. The dumb slot

was loaded in the proper position on the ground plane and successfully achieved the UWB frequency range. The MCP antenna provides an impedance bandwidth of 8.1 GHz and provides enhanced gains of 8.4 dBi and 8.2 dBi at 2.9 GHz and 9.1 GHz frequencies, respectively. Radiation patterns are observed semi-omnidirectionally and omnidirectionally in both E-plane and H-plane. To



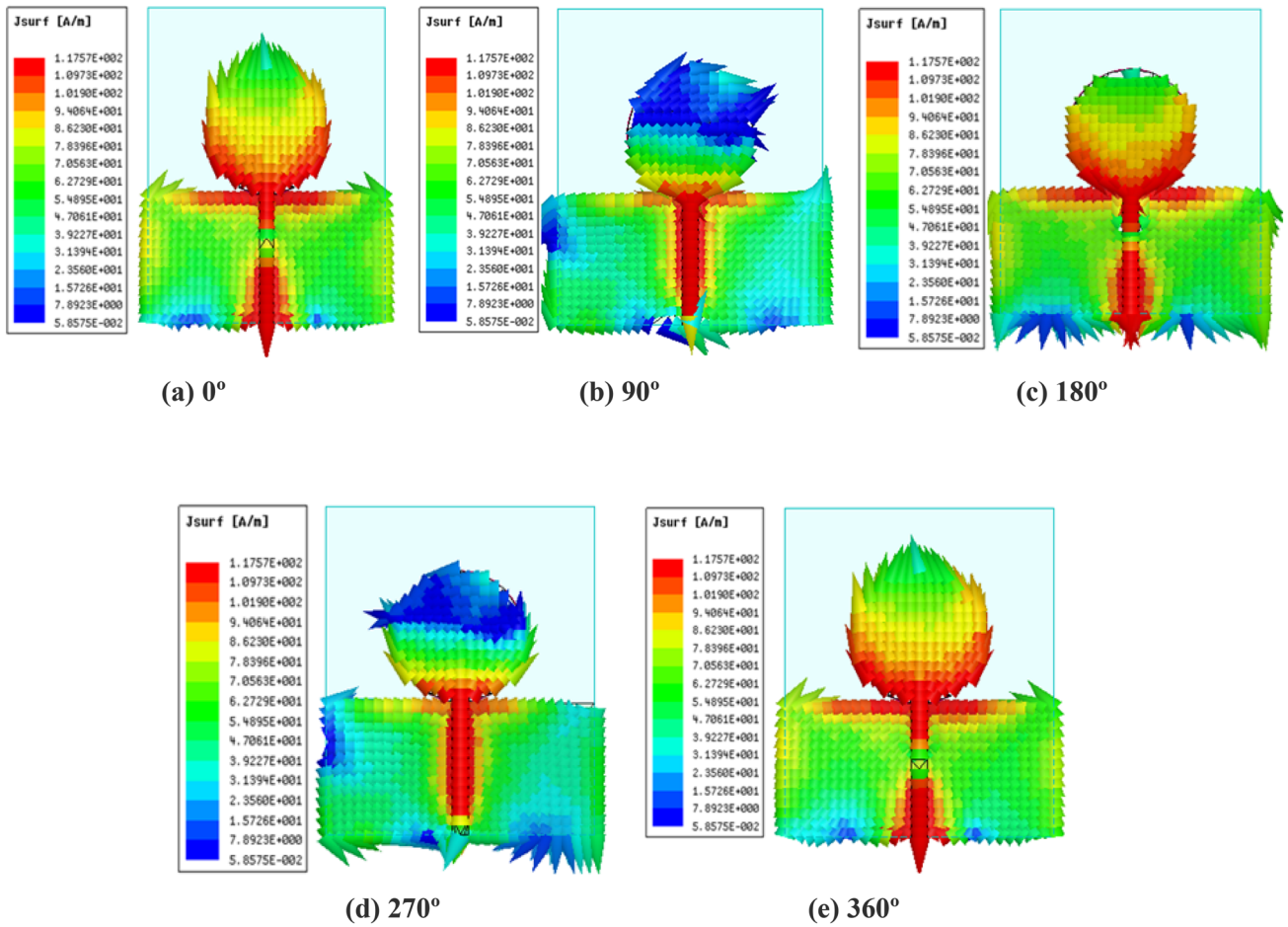
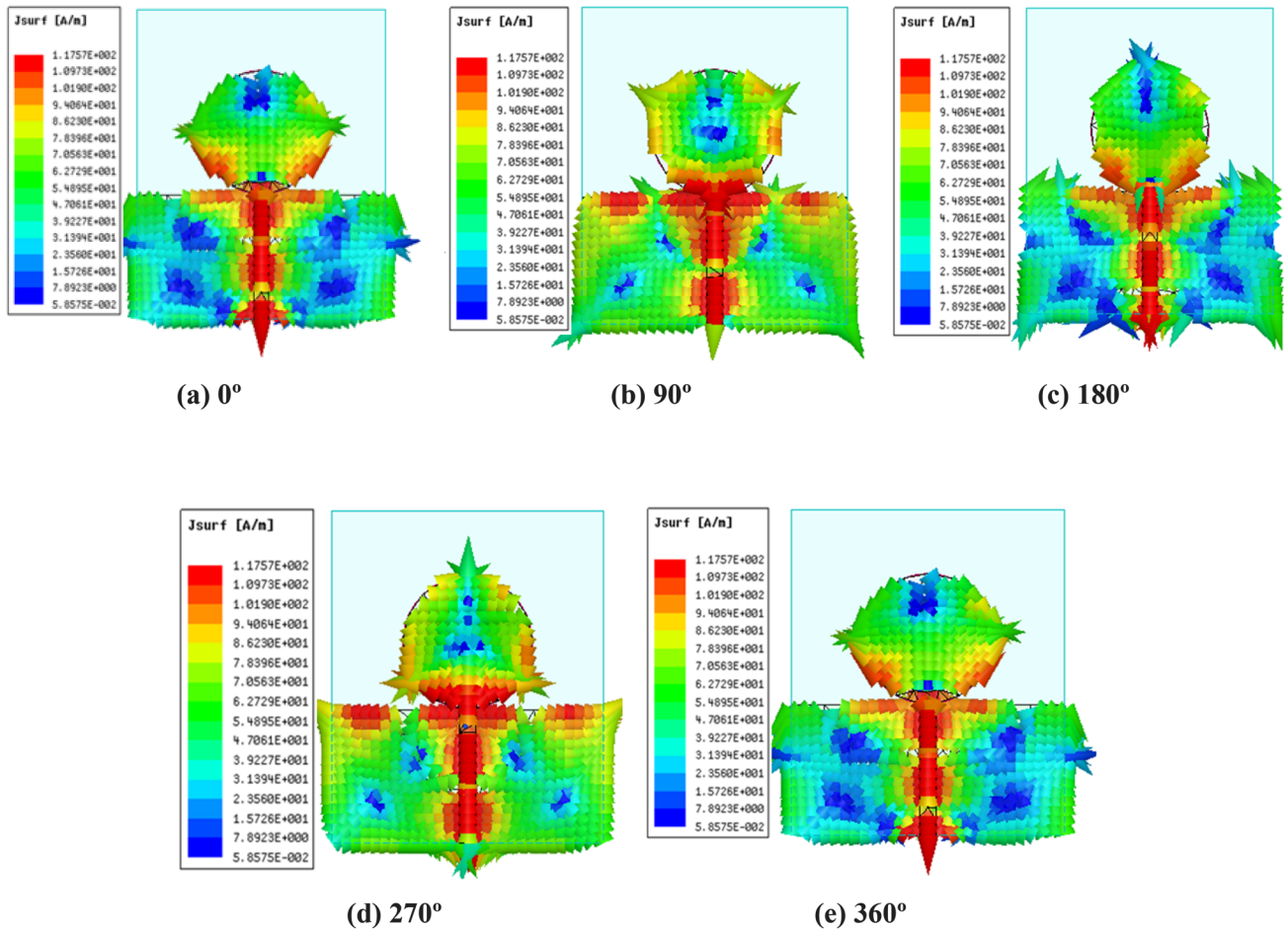


Fig. 14 Surface current intensity of the monopole circular-shaped patch antenna with different phase angles at 2.9 GHz



**Fig. 15** Surface current intensity of the monopole circular-shaped patch antenna with different phase angles at 9.1 GHz

confirm the effectiveness of the proposed antenna, these designs are simulated in HFSS, manufactured, and then measured using a vector network analyzer. According to the results obtained, the simulation and measurement are in good agreement. This is acceptable for individual

wireless systems. Therefore, this proposed antenna is a suitable application for UWB applications. The proposed MCP antenna can also be upgraded as a flexible antenna by considering the polyimide substrate material. The

**Table 3** Comparison of monopole circular– shaped patch antenna with other UWB antennas

Ref. no.	Antenna size (mm <sup>3</sup> )	Substrate Material	Reflection coefficient ( $S_{11}$ ) (dB)	Operating frequency bands (GHz)	Bandwidth (GHz)	Gain (dBi)
[4]	350×240×1.6	FR-4	< -10	4.5 9.5	9.2 (3.1–12.3)	4.2 6.8
[5]	50×42×1.5	FR-4	-33 -14.2 -23	3 6.5 9	7.47(2.69–10.16)	<8
[6]	30×30×1.6	FR-4	-26.5 -26	4.1 8.8	6 (4–10)	<5
[7]	70.45×46×0.8	FR-4	< -10	3 5 8	7.5(3.1–10.6)	-0.88 -2.36 1.54
[10]	28.1×17.1×1.4	FR-4	< -10	5.2 10.8 28.5	(4–40)	2.8
[11]	22×24×1.6	FR-4	< -10	3.4 7.5 9.8	8.2 (3–11.2)	≤5.4
[14]	50×42×1.5	FR-4	-33 -24	3 9	7 (2.78–9.78)	-
[20]	44×46×1.6	FR-4	-26.2 -24.3	4 7.8	10.87 (2.83–13.7)	2–5
[22]	42×24×1.6	FR-4	< -10	2.45 3.54	0.2 (2.3–2.5) 7.5 (3.1–10.6)	2–5
[23]	30×30×1.6	FR-4	< -10	3.5 4.5 7.8	9.82 (2.9–12.72)	1.2–5.3
Proposed MCP antenna	38×48×1.6	FR-4	-34.84	2.9	11.97 (2.33–14.3)	8.4
			-33.74	9.1		8.2

flexible MCP antenna will be useful for flexible communication devices and biomedical applications.

**Acknowledgements** The authors would like to thank for antenna design and testing facilities provided by Entuple Technologies Pvt. Ltd., Bangalore, India and the Department of ECE, K L University, Guntur, India.

### Compliance with ethical standards

**Conflict of interest** The authors declare that they have no conflict of interest.

**Open Access** This article is licensed under a Creative Commons Attribution 4.0 International License, which permits use, sharing, adaptation, distribution and reproduction in any medium or format, as long as you give appropriate credit to the original author(s) and the source, provide a link to the Creative Commons licence, and indicate if changes were made. The images or other third party material in this article are included in the article's Creative Commons licence, unless indicated otherwise in a credit line to the material. If material is not

included in the article's Creative Commons licence and your intended use is not permitted by statutory regulation or exceeds the permitted use, you will need to obtain permission directly from the copyright holder. To view a copy of this licence, visit <http://creativecommons.org/licenses/by/4.0/>.

### References

1. FCC (2002) Federal communications commission revision of Part 15 of the commission's rules regarding ultra-wideband transmission systems
2. Sami A, Rahman M, Bashir S (2019) Design of compact tri and quad band band-pass filters using stub loaded resonators for wireless applications. *SN Appl Sci* 1(9):1019
3. George R, Kumar C, Gangal S, Joshi M (2019) A low profile reconfigurable antenna for defense aircrafts. *SN Appl Sci* 1(6):608
4. Hossain M, Faruque MRI, Islam MT (2016) Design of a patch antenna for ultra wide band applications. *Microwave Opt Technol Lett* 58(9):2152–2156

5. Liang J, Chiau CC, Chen X, Parini CG (2005) Study of a printed circular disc monopole antenna for UWB systems. *IEEE Trans Antennas Propag* 53(11):3500–3504
6. Low Z, Cheong J, Law C (2005) Low-cost PCB antenna for UWB applications. *IEEE Antennas Wirel Propag Lett* 4:237–239
7. Ling C-W, Lo W-H, Yan R-H, Chung S-J (2007) Planar binomial curved monopole antennas for ultrawideband communication. *IEEE Trans Antennas Propag* 55(9):2622–2624
8. Wong K-L, Su S-W, Tang C-L (2005) Broadband omnidirectional metal-plate monopole antenna. *IEEE Trans Antennas Propag* 53(1):581–583
9. Dattatreya G, Kousalya K, Jyothirmayi Y, Krishna MV, Harsha D, Sri PAV, Naik KK Analysis of complementary split ring resonators on rectangular patch with inset feed for X-band application. In: 2017 International conference of Electronics, Communication and Aerospace Technology (ICECA), 2017. IEEE, pp 248–250
10. Saha TK, Goodbody C, Karacolak T, Sekhar PK (2019) A compact monopole antenna for ultra wideband applications. *Microwave Opt Technol Lett* 61(1):182–186
11. Azim R, Islam MT, Misran N (2011) Compact tapered-shape slot antenna for UWB applications. *IEEE Antennas Wirel Propag Lett* 10:1190–1193
12. Kaushal D, Shanmuganatham T, Sajith K Dual band characteristics in a microstrip rectangular patch antenna using novel slotting technique. In: 2017 international conference on intelligent computing, instrumentation and control technologies (ICICT), 2017. IEEE, pp 957–960
13. Gharakhili FG, Fardis M, Dadashzadeh GR, Ahmadi AKA, Hojjat N (2007) Circular slot with a novel circular microstrip open ended microstrip feed for UWB applications. *Prog Electromagn Res* 68:161–167
14. Liang J, Chiau C, Chen X, Parini C (2004) Printed circular disc monopole antenna for ultra-wideband applications. *Electron Lett* 40(20):1246–1247
15. Abedian M, Rahim S, Danesh S, Khalily M, Noghabaei S (2013) Ultrawideband dielectric resonator antenna with WLAN band rejection at 5.8 GHz. *IEEE Antennas Wirel Propag Lett* 12:1523–1526
16. Gatea KM (2012) Compact ultra wideband circular patch microstrip antenna. In: 2012 first national conference for engineering sciences (FNCES 2012), 2012. IEEE, pp 1–5
17. Kadam AA, Deshmukh AA, Deshmukh S, Doshi A, Ray KP (2019) Slit loaded circular ultra wideband antenna for band notch characteristics. In: 2019 national conference on communications (NCC), 2019. IEEE, pp 1–6
18. Karamanoğlu M, Abbak M, Şimşek S (2013) A planar ultra-wideband monopole antenna with half-circular parasitic patches. In: 2013 13th Mediterranean microwave symposium (MMS), 2013. IEEE, pp 1–4
19. Kumar N, Singh KK, Badhai RK (2016) A tapered feed circular monopole super ultra-wideband (UWB) printed antenna. In: 2016 international conference on communication and signal processing (ICCSP), 2016. IEEE, pp 1943–1946
20. Sayidmarie KH, Fadhel YA (2012) Design aspects of UWB printed elliptical monopole antenna with impedance matching. In: 2012 Loughborough antennas & propagation conference (LAPC), 2012. IEEE, pp 1–4
21. Nayna TFA, Haque E, Ahmed F (2016) Design of a X band defected ground circular patch antenna with diamond shaped slot and ring in patch for UWB applications. In: 2016 international conference on signal processing, communication, power and embedded system (SCOPE), 2016. IEEE, pp 559–562
22. Mishra SK, Gupta RK, Vaidya A, Mukherjee J (2011) A compact dual-band fork-shaped monopole antenna for Bluetooth and UWB applications. *IEEE Antennas Wirel Propag Lett* 10:627–630
23. Lu J-H, Yeh C-H (2012) Planar broadband arc-shaped monopole antenna for UWB system. *IEEE Trans Antennas Propag* 60(7):3091–3095
24. Rao PK, Singh KJ, Mishra R (2018) A circular shaped microstrip patch antenna for bluetooth/Wi-Fi/UWB/X-band applications. In: 2018 international conference on power energy, environment and intelligent control (PEEIC), 2018. IEEE, pp 638–641
25. Rodrigues EJ, Lins HW, D'Assunção AG (2014) Reconfigurable circular ring patch antenna for UWB and cognitive radio applications. In: The 8th European conference on antennas and propagation (EuCAP 2014), 2014. IEEE, pp 2744–2748
26. Safia OA, Omar A, Nedil M (2016) CPW-fed UWB antenna based on packing congruent circles in a circular patch. In: 2016 5th international conference on electronic devices, systems and applications (ICEDSA), 2016. IEEE, pp 1–3
27. Balanis CA (2016) *Antenna theory: analysis and design*. Wiley, New York
28. Khandelwal MK, Kanaujia BK, Kumar S (2017) Defected ground structure: fundamentals, analysis, and applications in modern wireless trends. *Int J Antennas Propag* 2017:1–22

**Publisher's Note** Springer Nature remains neutral with regard to jurisdictional claims in published maps and institutional affiliations.